A new gyrokinetic quasilinear transport model applied to particle transport in tokamak plasmas

C. Bourdelle, X. Garbet, F. Imbeaux, A. Casati, N. Dubuit, R. Guirlet, and T. Parisot

View Online   Export Citation
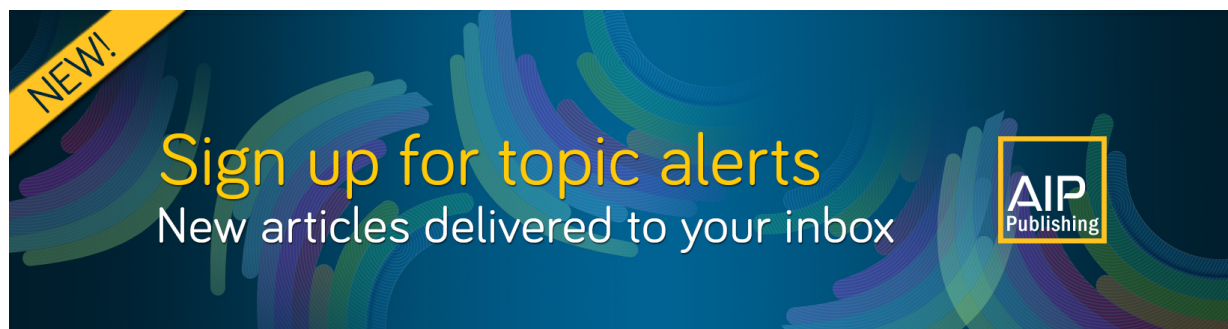
A new gyrokinetic quasilinear transport model applied to particle transport in tokamak plasmas

C. Bourdelle,[a] X. Garbet, F. Imbeaux, A. Casati, N. Dubuit, R. Guirlet, and T. Parisot
Association Euratom-CEA, CEA/DSM/DRFC, Centre de Cadarache, 13108 Saint-Paul-Lez-Durance, France

The scope of this paper is to present and benchmark the first version of a quasilinear calculation, QuaLiKiz, based on a fast linear gyrokinetic code, Kinezero [C. Bourdelle, X. Garbet, G. T. Hoang, J. Ongena, and R. V. Budny, Nucl. Fusion **42**, 892 (2002)] accounting for all unstable modes and summing over a wave-number spectrum. The fluctuating electrostatic potential frequency and wave-number spectra are chosen based on turbulence measurements and nonlinear simulations results. A peculiar focus on particle transport is developed. The directions of compressibility and thermodiffusion convections of ions and electrons are analytically derived for passing and trapped particles in both ion and electron turbulence. Also, the charge and mass dependence of trace heavy impurity convection is analytically estimated. These results are compared with quasilinear simulations done by QuaLiKiz. Finally, the impact of accounting for all unstable modes and of summing over the wave-number spectrum is shown to reverse in some cases the direction of particle fluxes. © *2007 American Institute of Physics*. [DOI: 10.1063/1.2800869]

I. INTRODUCTION

In order to better understand turbulent transport mechanisms and therefore enhance the predictive capability, actual available transport models have to be improved. Ideally, nonlinear gyrokinetic electromagnetic simulations for all species should be systematically performed. Unfortunately, for the coming 10 years, this approach is still too costly in terms of computer time.[1,2] A pragmatic tradeoff is to develop a quasilinear transport model based on a rapid linear gyrokinetic code (qualified here as a "gyrokinetic quasilinear transport model"). Other arguments are in favor of such an approach. Indeed, in a number of cases, the quasilinear approach exhibits a rather good agreement with experiments[3,4] and recently nonlinear gyrokinetic simulations have been shown to scale almost as quasilinear predictions.[5,6] Nevertheless, to correctly account for major nonlinear physics issues impacting turbulent transport (zonal flows,[7] turbulence spreading,[8,9] etc.), the quasilinear model should be refined thanks to extensive comparisons with nonlinear simulations, as already initiated in Refs. 6 and 10 but also thanks to more intensive confrontation with turbulence measurements.

Here, we present and benchmark the first version of a quasilinear calculation of heat and particle fluxes, QuaLiKiz, based on a fast linear electrostatic eigenvalue gyrokinetic code, Kinezero.[11] The most critical point, when estimating the quasilinear fluxes, is the choices made for the fluctuating electrostatic potential: its amplitude and its spectral shape versus both wave numbers and frequencies. For its amplitude, we use the recent work in Refs. 5, 12, and 13 for the spectral forms; we base our choices on turbulence measurements and nonlinear simulations. If compared to the recent TGLF quasilinear model,[6,10] the QuaLiKiz has the specificity to use a gyrokinetic code to calculate the growth rates,

whereas TGLF is based on a gyro-Landau fluid code. At a given wave number, QuaLiKiz has also the specificity of accounting for all unstable modes, since it is based on an eigenvalue code, whereas TGLF and the model proposed in Refs. 5, 12, and 13 account for the most unstable mode. Finally, as in TGLF, the sum over the wave-number spectrum is made rather than using the wave number at which the amplitude of the potential is maximal, as in Refs. 5, 12, and 13. The impact of these last two points is shown to be important, since it reverses the particle flux direction in some specific cases. After having introduced the new quasilinear gyrokinetic model, we illustrate the use of such a model to address a major transport issue in fusion devices, namely particle transport. Indeed, the fusion rate is directly influenced by particle transport: peaked density profiles for both D and T significantly increase it; on the contrary, He ash accumulation decreases it. Moreover, heavy impurity accumulation in the core leads to radiative collapse, whereas impurities, such as Ar or Ne, are welcome at the edge to create a radiative belt. Lately, significant efforts in understanding particle transport have been carried out on both theoretical and experimental levels. Turbulent particle transport has been shown to participate to both electron and impurity transport.[14–17] These are the reasons why we first focus on particle transport. In particular, we estimate analytically the direction of the particle fluxes for ions and electrons, in the case of curvature only and in the slab limit, for both electron and ion turbulence. We also discuss the dependence of the convection terms (thermodiffusion and compressibility) versus the charge and the mass of trace heavy impurities. Although a large part of these results has already been published,[18–20] here we aim at summarizing this information in three tables. QuaLiKiz is used to illustrate the change of direction of the particle flux expected by the analytical estimations. And we show that, as the impurity concentration

---

[a]Electronic mail: clarisse.bourdelle@cea.fr

increases, the analytical calculation valid for trace impurities no longer agrees with the numerical results.

In Sec. II, the quasilinear model is detailed and benchmarked. In Sec. III, the contributions to the quasilinear gyrokinetic particle flux are discussed both analytically and numerically. In Sec. IV, the impact of accounting for all unstable modes and for a wave-number spectrum on particle flux is illustrated. Finally, a summary and perspectives of this work are drawn in Sec. V.

II. A NEW GYROKINETIC QUASILINEAR MODEL: QUALIKIZ

A. The quasilinear gyrokinetic equation

The quasilinear gyrokinetic expression of the flux is the time average of the nonlinear Vlasov equation over a time τ larger than the characteristic time of the fluctuations $(1/\gamma)$ and smaller than the equilibrium evolution time (T_0), and where the fluctuating distribution function $(\widetilde{f})$ is assumed to respond linearly to the fluctuating potentials $(\widetilde{H})$ through the Vlasov equation. More details are given in Appendix A.

In the model presented here, the linearized Vlasov equation is computed by Kinezero[11] using the ballooning representation in a shifted circles geometry. Kinezero accounts only for electrostatic fluctuations. Two ion species and electrons are taken into account in both their trapped and passing domains. It is an eigenvalue code that computes all unstable modes. In Kinezero, the irreversibility is taken into account for trapped electrons since collisions are included,[21] for trapped ions since the integral in energy is done via Fried and Conte functions, and for the passing particle since the integrated expression is similar to the one given in Ref. 22, where it is also implicitly included. The eigenfunction of the electrostatic potential is a trial function chosen to be a Gaussian with a width that has been benchmarked against both GS2[23] and GYRO[24] as detailed in the Appendix of Ref. 21.

Hence, the quasilinear formulation leads to the following expressions for the particle and heat fluxes for each species s (respectively Γ_s and Q_s, Q_{Es} being the energy flux):[25]

$$
\begin{aligned}
\Gamma_s &= \left\langle \widetilde{n}_s \frac{ik_\theta \widetilde{\phi}}{B} \right\rangle \\
&= -\frac{n_s}{R}\left(\frac{q}{r}\right)^2 \frac{1}{B^2} \sum_{n,\omega} n^2 \left\langle \sqrt{\xi} e^{-\xi} \left[\frac{R\nabla n_s}{n_s} + \left(\xi - \frac{3}{2}\right) \frac{R\nabla T_s}{T_s} \right. \right. \\
&\quad \left. \left. + \frac{\omega}{n\omega_{Ds}} \right] \mathrm{Im}\left(\frac{1}{\omega - n\Omega_s(\xi,\lambda) + i0^+} \right) \right\rangle_{\xi,\lambda} |\widetilde{\phi}_{n\omega}|^2,
\end{aligned}
\tag{1}
$$

$$
\begin{aligned}
Q_{Es} &= \left\langle \frac{3}{2}\widetilde{P}_s \frac{ik_\theta \widetilde{\phi}}{B} \right\rangle \\
&= -\frac{n_s}{R}\left(\frac{q}{r}\right)^2 \frac{T_s}{B^2} \sum_{n,\omega} n^2 \left\langle \xi^{3/2} e^{-\xi} \left[\frac{R\nabla n_s}{n_s} + \left(\xi - \frac{3}{2}\right) \frac{R\nabla T_s}{T_s} \right. \right. \\
&\quad \left. \left. + \frac{\omega}{n\omega_{Ds}} \right] \mathrm{Im}\left(\frac{1}{\omega - n\Omega_s(\xi,\lambda) + i0^+} \right) \right\rangle_{\xi,\lambda} |\widetilde{\phi}_{n\omega}|^2.
\end{aligned}
\tag{2}
$$

The heat flux is[25]

$$
Q_s = Q_{Es} - \frac{3}{2}T_s \Gamma_s.
\tag{3}
$$

The integrands $\xi = (1/2 m_s V^2)/T_s$, $\lambda = \mu B(r,\theta=0)/(1/2 m_s V^2)$, $b = B(r,\theta)/B(r,0)$, with m_s the mass, V the velocity, μ the adiabatic invariant, B the magnetic field, and (r,θ,φ) the radial, poloidal, and toroidal coordinates. For trapped particles, the integral is

$$
\langle \cdots \rangle_{\xi,\lambda} = \int_0^{+\infty} \frac{2}{\sqrt{\pi}} d\xi \int_{\lambda_c}^1 d\lambda \frac{1}{4\bar{\omega}_2}
$$

and for passing,

$$
\langle \cdots \rangle_{\xi,\lambda} = \int_0^{+\infty} \frac{2}{\sqrt{\pi}} d\xi \int_0^{\lambda_c} d\lambda \frac{1}{4\bar{\omega}_2} \frac{1}{2} \sum_{\varepsilon_\parallel = \pm 1} \varepsilon_\parallel
$$

with $\bar{\omega}_2 = 1/\oint d\theta/2\pi 1/\sqrt{1-\lambda b}$ and $\lambda_c = \mu B(r,\theta=0)/\mu B(r,\theta=\pi)$.

The frequencies $n\omega_{Ds} = -k_\theta T_s/(e_s BR)$, $n\Omega_s = -k_\theta T_s/(e_s BR)\xi(2-\lambda b)f(\lambda)$ for trapped and $n\Omega_s = -k_\theta T_s/(e_s BR)\xi(2-\lambda b)f(\lambda) + \varepsilon_\parallel k_\parallel V_\parallel$ for passing, with $f(\lambda)$ a function of λ depending on the magnetic geometry: s (magnetic shear) and α [magnetohydrodynamic (MHD) parameter now included in Kinezero[26]], which differs for trapped and passing particles. For passing, $k_\parallel V_\parallel \approx \pm k_\theta w(s/q)(V_{Ts}/R)\sqrt{\xi}$, where n is the toroidal wave number, $k_\theta = nq/r$ is the poloidal wave vector, q is the safety factor, and s is the magnetic shear. And n_s is the density, T_s is the temperature, P_s is the pressure, and V_{Ts} is the thermal velocity. For more details concerning the notations, see Appendix A4 of Ref. 11.

B. Assumptions for the fluctuating electrostatic potential

The most delicate part in estimating the heat and particle fluxes using the quasilinear theory is due to the fact that the linearized gyrokinetic equation does not allow having information on the fluctuating electrostatic potential amplitude $|\widetilde{\phi}_{n\omega}|$ nor on its spectral shape versus the wave number n and the frequency ω.

Our choices are based on both nonlinear simulations results, since they provide the information on the potential amplitude and shape with n and ω, and on turbulence measurements of wave-number and frequency spectra.

1. Assumptions for the wave-number spectrum

Turbulence measurements performed by light scattering experiments[27] have shown that the density fluctuation $(\widetilde{n}/n)^2$ wave-vector spectrum scales as $e^{-4k\rho_i}$ above $k\rho_i = 0.5$, with k the wave vector and ρ_i the ion Larmor radius. Measurements by beam emission spectroscopy[28] showed the poloidal k_θ spectrum was symmetric around the value where the potential is maximal, $k_{\max}$. This symmetry is also shown by nonlinear simulations results for ion temperature gradient (ITG) modes, see, for example, Ref. 29, and for trapped electron modes (TEM).[30] Hence, we choose, from 0 to $k_{\max}$,

$$
|\widetilde{\phi}_{n\omega}|^2 \propto e^{4k_\theta \rho_i - 8k_{\max}\rho_i}
$$

and from $k_{\max}$ to infinity,

$$|\tilde{\phi}_{n\omega}|^2 \propto e^{-4k_\theta\rho_i}.$$

The maximum value of $|\tilde{\phi}_{n\omega}|^2$ at k_{max} is chosen such that the effective diffusivity, D_{eff}, follows the mixing length rule,

$$\max\left(D_{eff} \approx \frac{R\Gamma_s}{n_s}\right)\Bigg|_{k_{max}} = \frac{R}{n_s}\frac{k_\theta}{B}\frac{n_s e_s}{T_s}|\phi_{n\omega}^2|\Bigg|_{k_{max}}$$

$$= \frac{\gamma}{\langle k_\perp^2 \rangle}\Bigg|_{k_{max}}. \tag{4}$$

The choice for $\langle k_\perp^2 \rangle$ is based on both experimental observations and nonlinear simulation results. It should lead to a maximum $|\tilde{\phi}_{n\omega}|^2$ around $k_\theta\rho_i \approx 0.2$, i.e., lower than the linear stability prediction (typically $k_\theta\rho_i \approx 0.4$), as observed with BES[28] and in nonlinear simulations. It should also depend on q as observed in nonlinear simulations.[12,31] Recently, a pertinent choice for $\langle k_\perp^2 \rangle$ combining these two aspects was proposed in Refs. [5], [12], and [13]. Adding the impact of the MHD parameter, α, on the curvature drift to the expression proposed in Refs. [5], [12], and [13], one obtains for strongly ballooned modes

$$\langle k_\perp^2 \rangle = k_\theta^2[1 + (s-\alpha)^2\langle\theta^2\rangle] \tag{5}$$

with

$$\langle\theta^2\rangle = \frac{\int \theta^2|\phi_{n\omega}(\theta)|^2 d\theta}{\int |\phi_{n\omega}(\theta)|^2 d\theta}. \tag{6}$$

In Kinezero, $|\tilde{\phi}_{n\omega}|^2$ is a Gaussian trial eigenfunction[11] such that $\tilde{\phi}(\theta) \propto \sqrt{w}e^{-\theta^2 w^2/(2d^2)}$, where w is the mode width, determined in the fluid limit, and d is the distance between two resonating surfaces. The mode width has been compared to results given by GS2 and GYRO; see the Appendix of Ref. [21]. Therefore, here

$$\langle\theta^2\rangle = \frac{2d^2\Gamma(3/4)}{w^2\Gamma(1/4)}.$$

Here Γ denotes the mathematical Gamma function.

An example of the wave-number spectrum of $|\tilde{\phi}_{n\omega}|^2$ as chosen for our quasilinear model is shown in Fig. 1.

In the quasilinear model presented in Refs. [5], [12], and [13], the quasilinear fluxes are computed at a unique k_θ value, $k_\theta = k_{max}$, where $|\tilde{\phi}_{n\omega}|^2$ is maximal. In QuaLiKiz, we sum over the k_θ spectrum. In Sec. IV, we show that this difference can lead to substantial modification of the particle flux.

2. Assumptions for the frequency spectrum of the fluctuating potential

Now that the dependences of $|\tilde{\phi}_{n\omega}|$ with k_θ have been chosen, there remains the second delicate choice: the frequency spectrum shape. On this point as well, we will use both experimental evidence and theoretical results showing that the dependence of $|\tilde{\phi}_{n\omega}|$ with ω is not a delta function at frequency of the unstable mode, but rather a Lorentzian around this value. This enlargement is known as the turbulence broadening effect.

Measurements with light scattering diagnostics[32–34] show the enlargement of the frequency spectrum of density
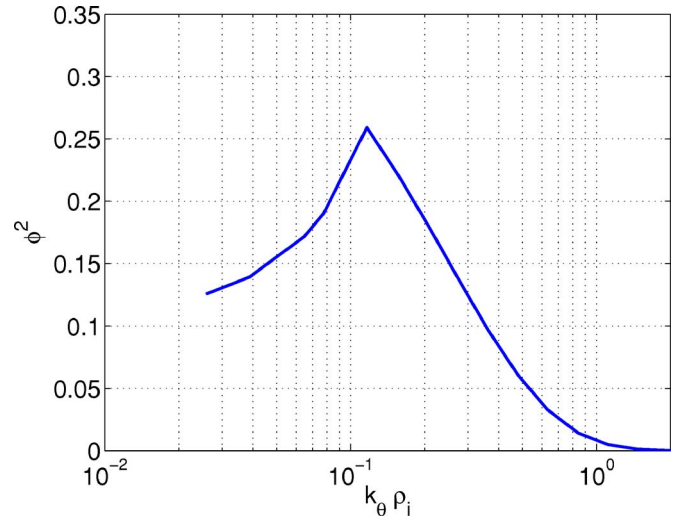

FIG. 1. (Color online) Example of the $|\tilde{\phi}_{n\omega}|^2$ k_θ spectrum as used in QuaLiKiz.

fluctuations, which is either Lorentzian or Gaussian. A theoretical explanation of the turbulence broadening expression is given in Ref. [35], where a Lorentzian around the frequency of the unstable modes is found. The turbulence broadening effect is taken into account in quasilinear models, such as the Weiland model[36] or GLF23.[4] In the latest work[5,12,13] building quasilinear fluxes based on the linear GENE or GS2 results, the issue of turbulence broadening is not explicitly mentioned. Nevertheless, in Ref. [19] on impurity transport, the existence of a parallel compressibility convection implies a Lorentzian choice for the ω spectrum of $|\tilde{\phi}_{n\omega}|$. In most existing quasilinear models (for a review, see Ref. [37]), the shape and the width of the frequency spectrum are not discussed in light of nonlinear simulation results and/or turbulence measurements.

In our model, we choose a Lorentzian shape with a width equal to the growth rate γ_0, hence

$$|\tilde{\phi}_{n\omega}|^2 = \frac{1}{\pi}\frac{\gamma_0}{(\omega - \omega_{r0})^2 + \gamma_0^2}|\phi_n|^2, \tag{7}$$

where ω_{r0} and γ_0 are, respectively, the real and imaginary parts of the eigenvalues of the linear gyrokinetic equation.

If it is reasonable to assume that the width increase is somewhat linked to the growth rate, it nevertheless remains arbitrary to choose a width strictly equal to γ_0. Moreover, experimental study of the scaling of the frequency spectrum width shows a broadening proportional to k_θ.[34] Our choice does not explicitly reproduce this tendency, although γ_0 goes like k_θ at low k_θ. Clearly more experimental analysis and comparison with results from nonlinear simulations are needed to clarify this point.

3. Benchmark of QuaLiKiz

In order to test our model, QuaLiKiz has been benchmarked against the model proposed in Refs. [5], [12], and [13] based on GS2.[23] Since GS2 ran linearly computes the most unstable mode only and is two orders of magnitude slower than Kinezero, to benchmark the two models, we have re-
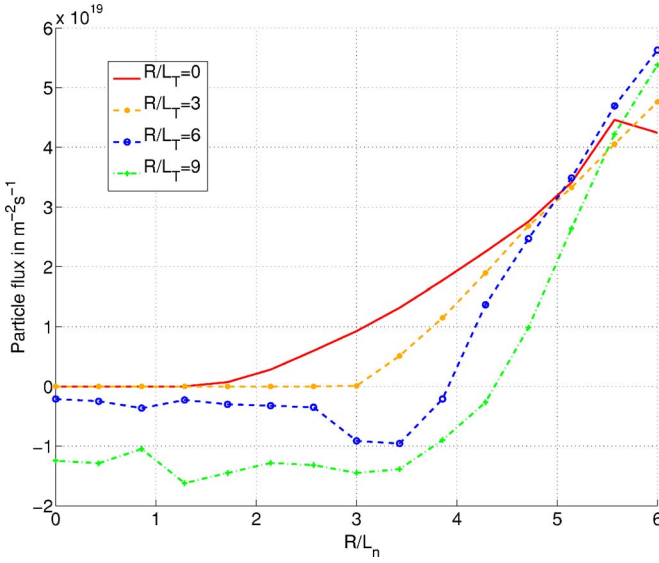
FIG. 2. (Color online) Particle flux calculated using Kinezero, for the most unstable mode and at $k=k_{\max}$ vs $R/L_n=-R\nabla n/n$ for four values of R/L_T.

duced the flux estimation in QuaLiKiz to the most unstable mode and to one value of k_θ, $k_\theta=k_{\max}$. The impact of summing over k_θ and accounting for all the unstable modes on particle fluxes is shown to reverse the direction of particle fluxes in some cases in Sec. IV. We have reproduced Fig. 3 of Ref. 13 where a normalized density gradient $R/L_n =-R\nabla n/n$ scan is performed for various values of the normalized temperature gradient $R/L_T=-R\nabla T_e/T_e=-R\nabla T_i/T_i$, with $T_e=T_i$, $Z_{\rm eff}=1$, $s=0.8$, $q=1.4$, $\alpha=0$, and $R/a=3$, $r/R =0.16$. The results obtained with this reduced version of QuaLiKiz are in qualitative agreement with the one published in Ref. 13; in particular, the particle fluxes reverse sign for the same values of $R/L_n=-R\nabla n/n$; see Fig. 2. The absolute values of the flux cannot be compared since a constant multiplier can be arbitrarily fixed in front of the flux. This constant should be fixed when comparing the model with experiments, and kept fixed from one experiment to another. This issue will be addressed when we integrate QuaLiKiz in a transport code. In the framework of a transport code, QuaLiKiz will be further compared with existing quasilinear transport models.

A second benchmark detailed in Appendix B is addressing the issue of the impact of collisions on particle flux. QuaLiKiz is found to be in qualitative agreement with Fig. 1 of Ref. 13, where the dependence of the particle flux versus collisionality is shown for the quasilinear GS2, GYRO, and GLF23.

To summarize, the first version of a new gyrokinetic quasilinear model, QuaLiKiz, has been presented and successfully benchmarked against Ref. 13. In the following, the results concerning particle flux are obtained with QuaLiKiz, as detailed above.

Nevertheless, some open issues remain: the proposed options for the saturation level and both the k_θ and ω spectra of $|\tilde{\phi}_{n\omega}|$ remain open issues. More detailed comparisons with turbulence measurements, such as the Doppler reflectometer recently installed in Tore Supra,[38] and with nonlinear simu-

lations should allow us to improve the assumptions made for the k_θ spectrum, the saturation level, and the frequency spectrum.

III. PARTICLE FLUX

As a first use of the new gyrokinetic quasilinear transport model presented in Sec. II, we propose to discuss in detail the particle flux. Recently, from both experimental and theoretical sides, particular attention has been paid to understanding the particle flux. The existence of a turbulent electron particle flux was demonstrated unambiguously in Ref. 14, where peaked electron density is explained by a dominant inward convection proportional to $\nabla q/q$.[15] In Asdex Upgrade, an outward convection has also been identified to be linked to a steeper electron temperature gradient.[39] For a review of these effects, see Ref. 40. The turbulent contribution to impurity transport is also expected to play a crucial role (for a review, see Ref. 16). For impurity transport, convection either directed inward or outward is expected to explain experimental results. These experimental results, for both electron and impurity transport, have been confronted with theoretical models based on nonlinear simulations[20,41,42] and on quasilinear simulations.[19,43] Two main convection mechanisms have been proposed: thermodiffusion and compressibility. Both can be either directed inward or outward. In the following, we will discuss in detail these terms in light of the quasilinear theory using both an analytical and a numerical approach.

A. Analytical estimation of diffusion and convection terms contributing to the particle flux

The quasilinear terms are derived analytically in a limit valid far from the instability threshold or for high Z_s trace impurities. Both electron and ion convection terms (thermodiffusion and compressibility) are derived, when the curvature is the only drift along the field line (trapped particles) and in the slab limit (passing electrons), and also for both electron and ion turbulence. The direction of the convection terms and the scaling of the trace heavy impurity flux with the charge and the mass of the ions are discussed and summarized in Tables I–III.

The contributions to the flux from diffusion, D_s, thermodiffusion, $C_s^{\rm th}$, and due to parallel and perpendicular compressibility, C_s^c, can be extracted from Eq. (1),

$$\Gamma_s = -\frac{n_s}{R}\left(\frac{q}{r}\right)^2\frac{1}{B^2}\sum_{n,\omega_0}n^2\left\langle\sqrt{\xi}e^{-\xi}\frac{\gamma_0}{(\omega-\omega_{r0})^2+\gamma_0^2}\left[\frac{R\nabla n_s}{n_s}\right.\right.$$
$$\left.\left.+\left(\xi-\frac{3}{2}\right)\frac{R\nabla T_s}{T_s}+\frac{\omega}{n\omega_{Ds}}\right]\delta(\omega-n\Omega_s(\xi,\lambda))\right\rangle_{\omega,\xi,\lambda}|\tilde{\phi}_n|^2$$
$$= -\frac{n_s}{R}\left(\frac{q}{r}\right)^2\frac{1}{B^2}\sum_{n,\omega_0}n^2\left\langle\sqrt{\xi}e^{-\xi}\frac{\gamma_0}{[n\Omega_s(\xi,\lambda)-\omega_{r0}]^2+\gamma_0^2}\right.$$
$$\left.\times\left[\frac{R\nabla n_s}{n_s}+\left(\xi-\frac{3}{2}\right)\frac{R\nabla T_s}{T_s}+\frac{n\Omega_s(\xi,\lambda)}{n\omega_{Ds}}\right]\right\rangle_{\xi,\lambda}|\tilde{\phi}_n|^2$$
$$= \frac{n_s}{R}\left(-D_s\frac{R\nabla n_s}{n_s}-C_s^{th}\frac{R\nabla T_s}{T_s}+RC_s^c\right), \tag{8}$$

TABLE I. Directions of the ion convection terms obtained in two quasilinear analytic limits: curvature only and slab.

	Ions			
	Compressibility		Thermodiffusion	
	Electron turbulence (TEM)	Ion turbulence (ITG)	Electron turbulence (TEM)	Ion turbulence (ITG)
Curvature only	Inward *Outward if $s \ll 0$ or $\alpha \gg 1$*		Inward *Outward if $s \ll 0$ or $\alpha \gg 1$*	Outward *Inward if $s \ll 0$ or $\alpha \gg 1$*
Slab limit	Outward	Inward	Inward	

where the resonance has been expressed thanks to the relation

$$\frac{1}{\omega + i\varepsilon - n\Omega_s(\xi,\lambda)} = -i\pi\delta(\omega - n\Omega_s(\xi,\lambda)). \quad (9)$$

Hence

$$D_s = \left(\frac{q}{r}\right)^2 \frac{1}{B^2} \sum_{n,\omega_0} n^2 \left\langle \frac{\sqrt{\xi}}{\sqrt{\pi}} e^{-\xi} \frac{\gamma_0}{[n\Omega_s(\xi,\lambda) - \omega_{r0}]^2 + \gamma_0^2} \right\rangle_{\xi,\lambda} |\tilde{\phi}_n|^2. \quad (10)$$

One can note that the diffusion term exists regardless of the assumption made concerning the frequency spectrum. Also, it does not depend on the charge number Z_s nor on the mass number, A_s, of the considered species, nor on the sign of the frequency of the unstable modes. The situation is quite different for the two convection terms.

The thermodiffusion term can be written as

$$C_s^{\text{th}} = \left(\frac{q}{r}\right)^2 \frac{1}{B^2} \sum_{n,\omega_0} n^2 \left\langle \sqrt{\xi} e^{-\xi} \left(\xi - \frac{3}{2}\right) \right.$$
$$\left. \times \frac{\gamma_0}{[n\Omega_s(\xi,\lambda) - \omega_{r0}]^2 + \gamma_0^2} \right\rangle_{\xi,\lambda} |\tilde{\phi}_n|^2. \quad (11)$$

Since $\langle \sqrt{\xi} e^{-\xi}(\xi - 3/2)\rangle_\xi = 0$, the thermodiffusion term exists if, and only if, a frequency spectrum expression depending on energy is included. In our case, the assumption made for the frequency spectrum [Eq. (7)], where Eq. (9) implies $\omega = n\Omega_s(\xi,\lambda)$, leads to a nonzero thermodiffusion term as given

in Eq. (11). Hence the behavior of this term depends strongly on the choice made for this spectrum. It is not the case for the compressibility term, which can be expressed as

$$RC_s^c = -\left(\frac{q}{r}\right)^2 \frac{1}{B^2} \sum_{n,\omega_0} n^2$$
$$\times \left\langle \sqrt{\xi} e^{-\xi} \frac{n\Omega_s(\xi,\lambda)}{n\omega_{Ds}} \frac{\gamma_0}{[n\Omega_s(\xi,\lambda) - \omega_{r0}]^2 + \gamma_0^2} \right\rangle_{\xi,\lambda} |\tilde{\phi}_n|^2 \quad (12)$$

and exists even without accounting for turbulence broadening since $\langle \sqrt{\xi} e^{-\xi}\rangle_\xi \neq 0$.

To understand the parametric dependences of these terms analytically, we will consider two simplified cases. First, we consider the curvature drift only, i.e., $n\Omega_s = -k_\theta T_s/(e_s BR)\xi(2 - \lambda b)f(\lambda)$, which is the case for trapped particles. Second, we will consider a slab case in which $n\Omega_s = k_\parallel V_\parallel$, which is close to the case of passing electrons since their thermal velocity is higher than the curvature drift, but is rather extreme for passing ions. All details concerning the analytical derivation are given in Appendix C.

In the case of curvature drift only, to derive analytical expressions, we assume $\omega_{r0} \gg n\omega_{Ds}$, which is valid far from the instability threshold or for high Z_s trace impurities. The curvature compressibility term reduces to a curvature inward pinch, the existence of which does not depend on the choice made for the frequency spectrum, as already shown by Turbulence EquiPartition theories.[18,44] It does not depend on the

TABLE II. Directions of the electron convection terms obtained in two quasilinear analytic limits: curvature only and slab.

	Electrons			
	Compressibility		Thermodiffusion	
	Electron turbulence (TEM)	Ion turbulence (ITG)	Electron turbulence (TEM)	Ion turbulence (ITG)
Curvature only	Inward *Outward if $s \ll 0$ or $\alpha \gg 1$*		Outward *Inward if $s \ll 0$ or $\alpha \gg 1$*	Inward *Outward if $s \ll 0$ or $\alpha \gg 1$*
Slab limit	Inward	Outward	Inward	

TABLE III. Dependences of trace heavy impurities convection terms vs their charge and mass numbers obtained in the quasilinear analytic limit.

	Heavy trace impurities	
	Compressibility	Thermodiffusion
Curvature only	No dependences	Scales as $1/Z_s$
Slab limit	Scales as Z_s/A_s	Scales as $1/A_s$

charge nor on the background turbulence. It is directed inward, unless s is strongly negative and/or α large enough to reverse the sign of $\langle f(\lambda)\rangle_\lambda$, in which case the curvature convection can be outward. On the contrary, the convection due to thermodiffusion exists if, and only if, the frequency spectrum depends on energy. Its sign depends on the sign of the product $n\omega_{Ds}\omega_{r0}\langle f(\lambda)\rangle_\lambda$. In the case of ion turbulence (electron turbulence), it is directed outward for ions (electrons) and inward for electrons (ions).[41] *Nota Bene*, as for the curvature compressibility, it reverses direction if the sign of $\langle f(\lambda)\rangle_\lambda$ reverses, hence if the magnetic shear is strongly negative or the MHD Shafranov parameter, α, is large enough. For high Z_s trace impurities, the scaling with respect to the charge follows a $1/Z_s$ dependence as found previously.[18,20]

In the "slab limit," where the curvature is neglected, $n\Omega_s = k_\parallel V_\parallel \approx \pm k_\theta w (s/q)(V_{Ts}/R)\sqrt{\xi}$. For the analytical derivation, we assume that $\omega \gg k_\parallel V_\parallel$, which is reasonable for heavy impurities, but rather a strong assumption for light ions and electrons. As in the "curvature only" case, the thermodiffusion convection exists if, and only if, the frequency spectrum depends on energy. Its direction is always inward. It scales as s^2 and as $1/A_s$ for trace impurities. Contrary to the curvature compressibility term, and as with the thermodiffusion, the parallel compressibility contributes to the flux only if one accounts for a frequency spectrum depending on energy. The sign of the parallel compressibility depends both on the sign of the charge of the considered species and on the direction of the modes. For turbulence in the electron (ion) drift direction, the compressibility is directed inward for electrons (ions) and outward for ions (electrons). These directions are opposite to the thermodiffusion convection of trapped particles. This parallel compressibility term scales like Z_s/A_s, so at fixed mass, it is stronger for a higher charge species. These results were shown previously in Ref. 19.

Three tables summarize the convection terms characteristics in the limits considered above: far from the instability threshold or for heavy trace impurities. Tables I and II summarize the direction of each term, respectively for ions and electrons and depending on the direction of the drift given by the dominant instability. Table III summarizes the scaling of the trace impurity convective terms with the impurity charge and mass. To complete this summary, we recall that only the curvature compressibility convection exists without accounting for a frequency spectrum depending on energy. The parallel compressibility and the thermodiffusion terms could both be modified by another choice of the frequency spectrum. One should also recall that, if the "curvature only" case

is valid for trapped species, for passing species both "curvature only" and "slab limit" contribute to the computed convection terms.

B. Illustration of diffusion and convection terms from QuaLiKiz

Thanks to the review of the analytical simplified quasilinear particle flux, it is easier to interpret results from QuaLiKiz on both the direction of convective terms and the charge and mass dependences of the impurity fluxes. We show that if broad qualitative agreement is found with the analytical approach, only a numerical simulation can give more quantitative information needed to interpret experimental data.

1. Direction of the convective terms

To illustrate the directions of the convective terms of particle transport, we scan the ion temperature gradient in order to pass from a pure TEM to a dominated ITG regime; crossing a mixed ITG-TEM zone, $R/L_{Ti} = -R\nabla T_i/T_i$ is varied from 0 to 7 with $R/L_n = -R\nabla n/n = 0$ and $R/L_{Te} = -R\nabla T_e/T_e = 9$ fixed. The other parameters are $T_e = T_i$, $s = 0.8$, $q = 1.4$, $\alpha = 0$, $R/a = 3$, $r/R = 0.16$, and $Z_{eff} = 2$ with a mix of D and C.

The diffusion and convection terms (thermodiffusion C_s^{th} and compressibility RC_s^c) are illustrated in Fig. 3 for passing and trapped electrons, D and C.

Diffusion is always directed outwards. As expected, thermodiffusion is inward for passing electrons, since the slab limit is valid in this case, and outward for trapped electrons since the TEM are the dominant modes. Thermodiffusion on ions, both trapped and passing, is found to reverse direction and to be inward when ITG are not yet destabilized and outward for higher ion temperature gradients, as predicted by the analytical calculation. The inward thermodiffusion found for the slab branch is not visible on passing ions, because, contrary to passing electrons, the curvature drift frequency is of the order of $k_\parallel V_\parallel$ for passing ions. The compressibility term is always directed inward for trapped particles, as expected from the curvature pinch. On passing particles, the contribution of the parallel compressibility is clearly identified. For passing ions, it reverses direction from outward to inward as the ion temperature gradient increases; the reversal is around $R/L_{Ti} = 4$. For passing electrons, it switches from inward to outward at $R/L_{Ti} = 6$.

In this case, the approximations used for the analytical calculation give the correct qualitative behaviors of the various convective terms. Nevertheless, the value of R/L_{Ti} at which the direction of the convection changes sign can only be obtained thanks to numerical calculations.

2. Scaling of impurity fluxes

Concerning the scaling of trace heavy impurities with their charge and mass, the behavior estimated by our analytical approach is tested against QuaLiKiz simulations for Tore Supra experiments in Ref. 45.

Nevertheless, for lighter impurities, the approximation $\omega_{r0} \gg n\omega_{Ds}$ is no longer valid and it remains difficult to qualitatively predict the direction of impurities as their concentra-
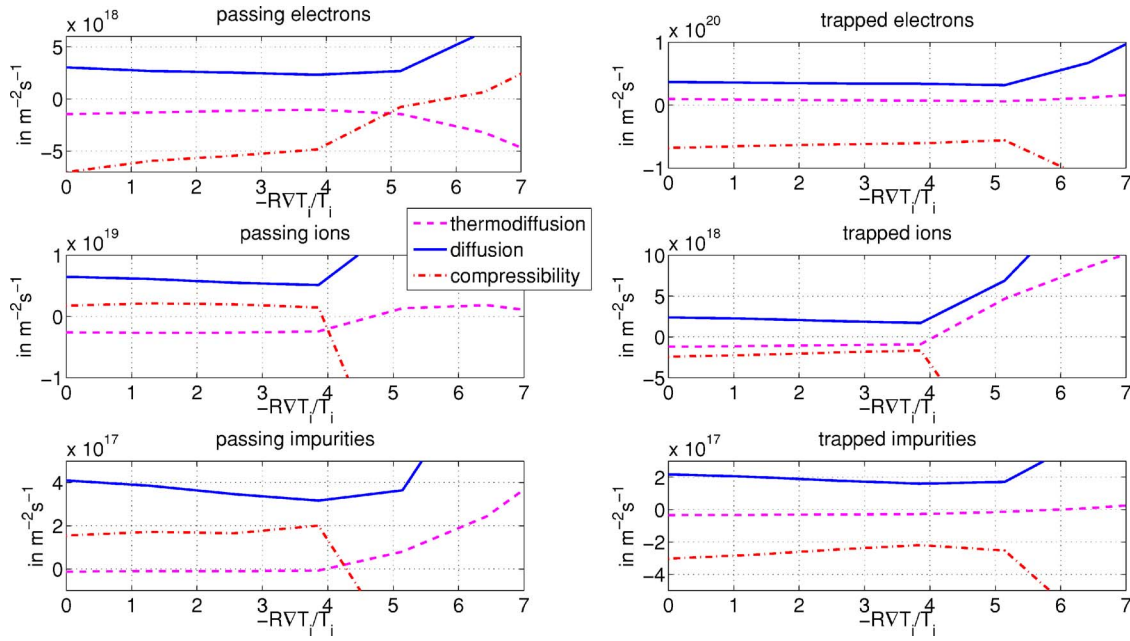
FIG. 3. (Color online) Diffusion, n_s/RD_s, full line; thermodiffusion, n_s/RC_s^{th}, dashed line; compressibility, $n_sC_s^c$, dot-dashed line vs $R/L_{Ti}=-R\nabla T_i/T_i$: for electrons, passing and trapped; ions, here D, passing and trapped; impurities, here C, passing and trapped.

tion increases and starts having an impact on the turbulence itself. To illustrate this difficulty, we show in Fig. 4 the C flux versus the concentration of C for four types of turbulence: both ion and electron turbulence $(R/L_{Ti},R/L_n,R/L_{Te})=(9,3,9)$, ion turbulence $(R/L_{Ti},R/L_n,R/L_{Te})=(9,0,0)$, electron turbulence $(R/L_{Ti},R/L_n,R/L_{Te})=(0,3,0)$, and $(R/L_{Ti},R/L_n,R/L_{Te})=(0,0,9)$, with $T_e=T_i$, $s=1$, $q=2$, $\alpha=0$, $R/a=3$, and $r/R=0.16$. For the ion turbulence case, the flux direction reverses as the C concentration is increased, and for the elec-

tron turbulence driven by density gradient the increase of C concentration leads to a complete stabilization of the modes. For the other two cases, the direction is not modified, only the amplitude is affected by higher concentration.

To summarize this section, two different mechanisms can modify the direction of the convection: for passing particles, the parallel compressibility, and for passing and trapped particles, the thermodiffusion. On the other hand, the curvature pinch acting on all particles is always directed inward. Moreover, for a given type of instability, parallel compressibility and thermodiffusion have opposite directions, hence knowing precisely the direction of the turbulence, and the amplitude of both types of convection, is important. These mechanisms are found analytically and confirmed with QuaLiKiz. But it is clear that the total convection term is a delicate equilibrium between the various contributions, and that only a numerical precise calculation can predict the convection direction. Moreover, other choices made for the quasilinear flux calculation can reverse the directions of the convection such as the sum over k_θ and the sum over all unstable modes. These impacts are detailed in Sec. IV.

IV. IMPACT OF SUMMING OVER k_θ AND OVER ALL UNSTABLE MODES ON PARTICLE FLUX

In this section, the specificities of the quasilinear calculations made in QuaLiKiz are discussed. It is shown that the particle flux direction can be modified when summing over all unstable modes. Also, it is proven that, summing over the k_θ spectrum, instead of accounting for one single k_θ, can change the direction of the fluxes.

A. Impact of summing over k_θ

To illustrate the impact of summing over k_θ, we choose to run a case similar to the scan proposed in Ref. 19 domi-
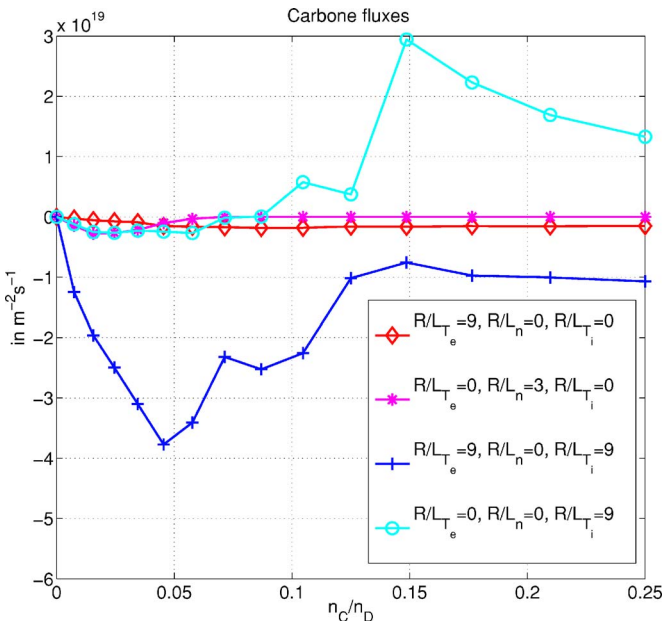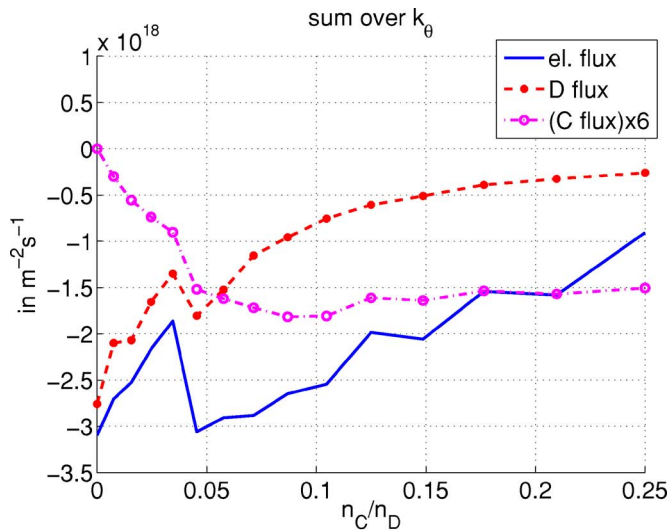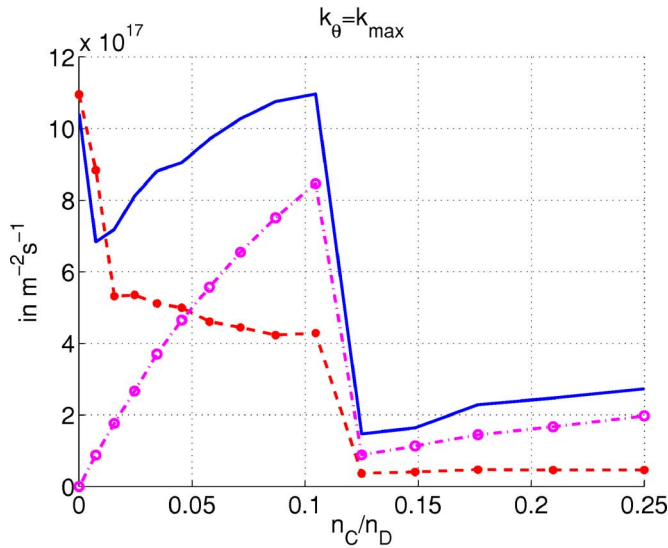

FIG. 4. (Color online) C fluxes vs n_C/n_D for four types of turbulence: diamonds, electron turbulence driven by R/L_{Te}; asterisks, electron turbulence driven by R/L_{ne}; crosses, both ion and electron turbulences; circles, ion turbulence.

(a)

(b)

FIG. 5. (Color online) electron, main ion (D), and impurity (C) particle fluxes vs the C concentration: n_C/n_D. (a) When summing over k_θ as done in QuaLiKiz; (b) for the case in which $k_\theta=k_{max}$ as proposed in Refs. 5, 12, and 13.

FIG. 6. (Color online) Passing C particle flux vs $k_\theta\rho_i$, for low C concentration: $n_C/n_D=0.01$.

nated by electron heating, i.e., $(R/L_{Ti},R/L_n,R/L_{Te})$ $=(0,0,9)$, with $T_e=T_i$, $s=1$, $q=2$, $\alpha=0$, $R/a=3$, and $r/R=0.16$.

In the example illustrated in Fig. 5, the impact of summing or not over k_θ is rather dramatic. Indeed, all fluxes are directed outward when accounting for one $k_\theta=k_{max}$ as proposed in Refs. 5, 12, and 13 and they are all directed inward when summing over k_θ as done in QuaLiKiz. Indeed, as illustrated in Fig. 6, passing impurities can be directed outward at low k_θ but their direction can reverse at higher k_θ, leading to an overall reduced outward flux due to passing impurities, as in this case, or even to an inward flux.

Hence, when summing over k_θ, the outward flux induced by passing impurities is reduced and is weaker than the inward flux carried by trapped impurities, leading to an overall inward impurity flux. This illustrates the importance of the
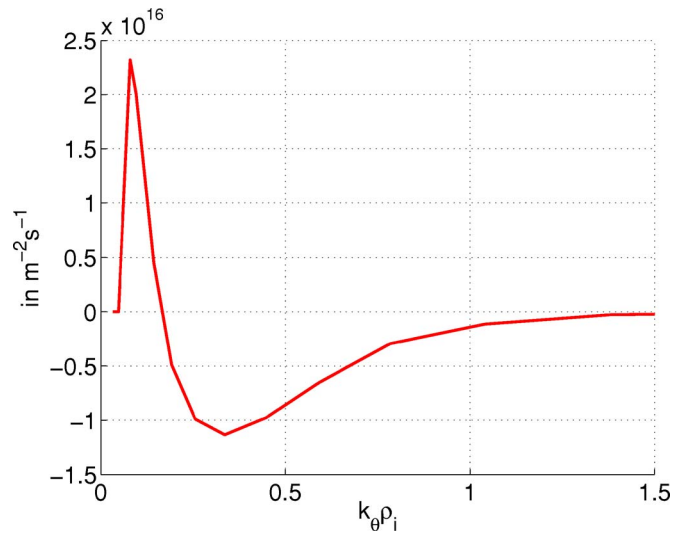
balance between passing and trapped particle fluxes, which strongly depends on the fraction of trapped particles, hence on the radial location.

In light of these results, the outward impurity flux identified in Ref. 19 to be a candidate to explain the JET electron heated experiments should be revisited.

B. Impact of summing over all unstable modes

In Fig. 7, for the same set of parameters as for Fig. 3, except for a wider extension of $R/L_{Ti}=-R\nabla T_i/T_i$ from 0 to 18, the particle fluxes of the two ions (D and C) and of electrons are compared when all unstable modes contribute as done in QuaLiKiz [Fig. 7(a)], and when only the most unstable modes contribute to the fluxes, as done in Refs. 5, 12, and 13 and in Refs. 6 and 10 [Fig. 7(b)], but here for both cases the sum over k_θ is done.

The most striking differences between these two cases can be observed on the impurity fluxes between $R/L_{Ti}=5$ and 13. It corresponds to a range of gradients where two unstable modes coexist. For example, for $R/L_{Ti}=9$, the most unstable mode goes in the ion drift direction, and the other goes in the electron drift direction, as shown in Fig. 8.

To summarize, we have shown here that it is necessary to account for a k_θ spectrum for the fluctuation electrostatic potential. Indeed, for passing particles the flux can reverse sign at k_θ higher than k_{max}, and in some cases the flux, when summed over k_θ, can be of the opposite sign than the flux at k_{max}. Also, when more than one mode is unstable, accounting for all unstable modes can reverse the direction of the flux; in our example, the impurity flux changed sign.

V. CONCLUSIONS AND PERSPECTIVES

With the aim of improving first-principles-based transport models used in integrated transport codes, we propose a new quasilinear gyrokinetic model, QuaLiKiz. QuaLiKiz is based on a fast linear eigenvalue gyrokinetic code, Kinezero.[11] The k_θ and frequency spectra chosen for the fluc-
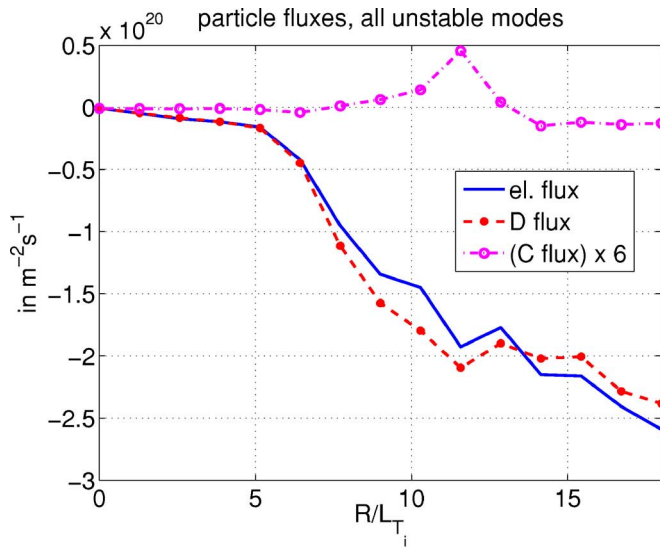
(a)
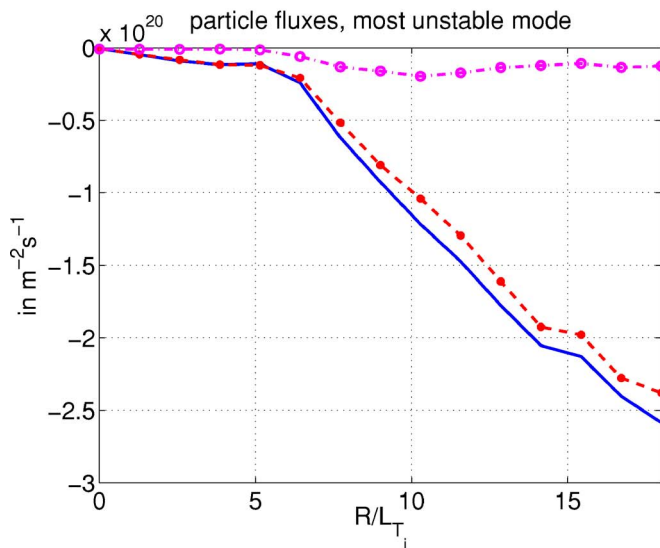
(b)

FIG. 7. (Color online) Electron flux, full line; D flux, dashed line with asterisks; C flux, dot-dashed line with circles vs $R/L_{Ti}=-R\nabla T_i/T_i$. (a) When only the most unstable mode contribute to the fluxes; (b) when all unstable modes contribute.

FIG. 8. (Color online) Growth rates and frequencies of the two unstable modes at $R/L_{Ti}=9$.

tuating electrostatic potential are based on turbulence measurements and nonlinear simulations results. QuaLiKiz has been successfully benchmarked against the quasilinear model based on GS2 proposed in Refs. 5, 12, and 13. If compared with TGLF,[6,10] QuaLiKiz is based on linear gyrokinetic code whereas TGLF is based on gyro-Landau fluid equations, QuaLiKiz accounts for all unstable modes versus the most unstable mode in TGLF, and the k_θ spectrum and the saturation levels are chosen differently. Also, contrary to the model proposed in Refs. 5, 12, and 13, QuaLiKiz accounts for all unstable modes and sums the flux over a k_θ spectrum. These two specificities are shown to be important, since they can reverse the particle flux direction. Hence, QuaLiKiz has some distinctive features that make it a valuable code to be compared to others in order to improve transport models for integrated modeling.
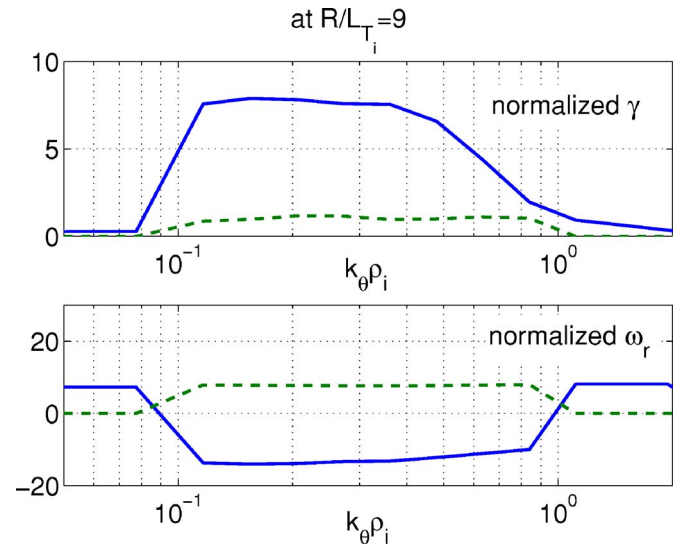
Concerning particle transport, analytical quasilinear estimations of the gyrokinetic fluxes are found to give good qualitative behavior of the convection direction. The compressibility convection due to curvature is directed inward, and does not depend on the chosen frequency spectra. On the contrary, the thermodiffusion and parallel compressibility convections exist only if a frequency spectrum depending on energy is included in the model. These convections also change direction depending on the nature of the background turbulence, and they have opposite directions. Numerical simulations done with QuaLiKiz are in qualitative agreement with the analytical predictions. Nevertheless, only a numerical simulation can conclude on the direction of the convection, since the nature of the turbulence is important and since the final flux is the result of a delicate equilibrium between convection terms having opposite directions and carried diversely by passing and trapped particles. Concerning the impurity convection, we show that the analytical dependences found for trace impurity are usually not extrapolatable to higher impurity concentration.

To further test the validity of the quasilinear approach, wider confrontations between nonlinear simulations and turbulence measurements are needed, in particular to improve the choices made for the k_θ and frequency spectra of the fluctuating potential. Efforts should also be carried out to model the impact of nonlinear structures such as streamers or zonal flows,[10] as well as the turbulence spreading phenomena. Hence, building always better first-principles-based transport models requires more confrontation between nonlinear simulation results and turbulence measurements.

Since QuaLiKiz is based on a fast linear gyrokinetic solver, we foresee using this model directly in time-dependent integrated simulations as a quantitative predictive tool.

APPENDIX A: DERIVATION OF THE QUASILINEAR FLUX

f is the distribution function and H the Hamiltonian. The fluctuations $(\tilde{f}, \tilde{H})$ are assumed to be significantly smaller than the equilibrium quantities (f_0, H_0) such that

$$f = f_0 + \tilde{f}, \quad H = H_0 + \tilde{H}. \tag{A1}$$

Averaging over τ, the Vlasov equation leads to

$$\int_0^\tau \frac{dt}{\tau} \frac{df}{dt} \approx \frac{\partial f_0}{\partial t} - \int_0^\tau \frac{dt}{\tau} [\tilde{H}, \tilde{f}] = 0 \tag{A2}$$

with α the angle variables and $\vec{J}$ the action variables, and knowing that f_0 depends only on $\vec{J}$, one obtains

$$\frac{\partial f_0}{\partial t} - \int_0^\tau \frac{dt}{\tau} \int_0^{2\pi} \frac{d^3\alpha}{(2\pi)^3} \left(\frac{\partial \tilde{H}}{\partial \alpha} \frac{\partial \tilde{f}}{\partial \vec{J}} + \tilde{f} \frac{\partial \tilde{H}}{\partial \vec{J} \partial \alpha} \right) = 0. \tag{A3}$$

Therefore, the flux, Γ, carried by f is given by

$$\frac{\partial f_0}{\partial t} + \nabla_{\vec{J}} \cdot \Gamma = 0 \tag{A4}$$

with

$$\Gamma = - \int_0^\tau \frac{dt}{\tau} \int_0^{2\pi} \frac{d^3\alpha}{(2\pi)^3} \tilde{f} \frac{\partial \tilde{H}}{\partial \alpha}. \tag{A5}$$

The three action variables are linked to the following conserved quantities: the adiabatic invariant of the cyclotronic motion, the energy of the guiding center, and the toroidal angular momentum. $\tilde{f}$ and $\tilde{H}$ are periodic versus the angle variables, and can be expressed thanks to Fourier sums where ω is the frequency and $\vec{n}$ is the wave number of the mode,

$$\tilde{f} = \sum_{\vec{n}, \omega} f_{\vec{n}\omega}(\vec{J}) e^{i(\vec{n}\cdot\alpha - \omega t)}, \tag{A6}$$

$$\tilde{H} = \sum_{\vec{n}, \omega} H_{\vec{n}\omega}(\vec{J}) e^{i(\vec{n}\cdot\alpha - \omega t)}. \tag{A7}$$

Implementing these expressions in Eq. (A5) leads to

$$\Gamma = - i\vec{n} \int_0^\tau \frac{dt}{\tau} \int_0^{2\pi} \frac{d^3\alpha}{(2\pi)^3} \tilde{f} \tilde{H}. \tag{A8}$$

Now, we assume that the nonlinear term $\tilde{f}\tilde{H}$ is constant over the time τ, hence

$$\Gamma \approx \sum_{\vec{n}, \omega} i\vec{n} \tilde{H}^*_{\vec{n}\omega} \tilde{f}_{\vec{n}\omega}, \tag{A9}$$

meaning that τ is much larger than the linear growth time and that nonlinear interactions, such as zonal flows or streamers, do not occur during this time. Hence ω is real. Nevertheless, the linear growth rate γ will play a role in the choice of the fluctuating potential to scale its saturation level and its frequency spectrum.

Finally, we assume that $\tilde{f}$ linearly responds to $\tilde{H}$ through the linearized Vlasov equation, therefore
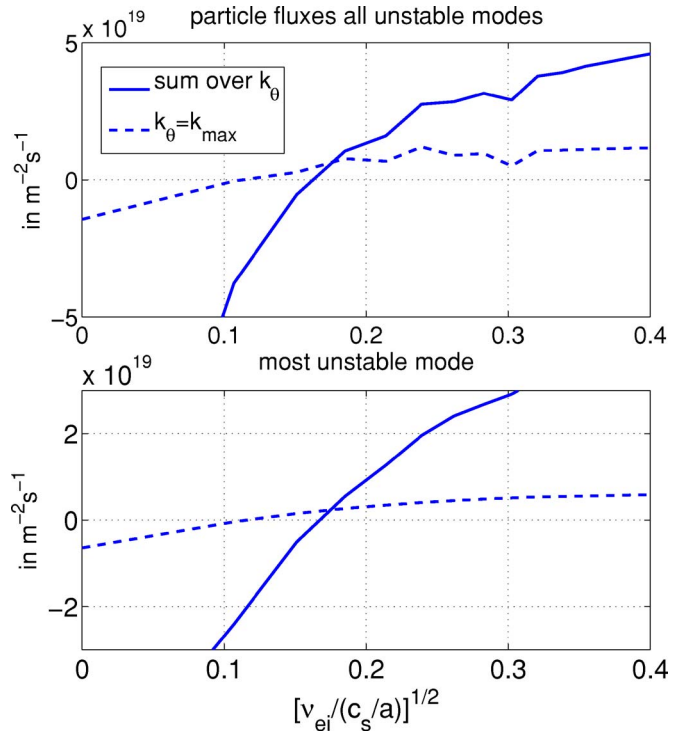

FIG. 9. (Color online) The particle flux as a function of collisionality, computed with QuaLiKiz, for the case in which all unstable modes are accounted for and the most unstable modes contribute. Full line: the flux is obtained by a sum over the k_θ spectrum; dashed line: only $k_\theta = k_{max}$ contributes to the flux.

$$\Gamma = \sum_{\vec{n}, \omega} \vec{n} \, \text{Im} \left(\frac{\vec{n} \cdot \partial_{\vec{J}} f_0}{\omega - \vec{n} \cdot \Omega(\vec{J}) + i0^+} \right) |\tilde{H}_{\vec{n}\omega}|^2, \tag{A10}$$

where $\Omega(\vec{J}) = d_t \alpha$ and $i0^+$ is the Landau prescription insuring the irreversibility of the equation implying the systematic existence of at least a very small imaginary quantity at the denominator.

In our case, we have used the gyro-averaged Vlasov equation to compute the fluxes. We have qualified the fluxes as "gyrokinetic quasilinear fluxes."

APPENDIX B: ADDITIONAL BENCHMARK OF QUALIKIZ

A second benchmark is addressing the issue of the impact of collisions on particle flux. The impact of collisions on trapped electrons has been included in Kinezero using a Krook operator as detailed in Ref. 21. The comparison is done with Fig. 1 of Ref. 13, where the dependence of the particle flux versus collisionality is shown for the quasilinear GS2, GYRO, and GLF23. QuaLiKiz gives the same qualitative results as GS2_QL, GYRO, and GLF23, i.e., the sign of the particle flux reverses as the electron collisionality is increased. If the sum over all k_θ is performed, then the flux reverses direction at $[\nu_{ei}/(c_s/a)]^{1/2} = 0.16$, between GYRO and GLF23, Fig. 9. If the fluxes are estimated at k_{max}, then the threshold is found at 0.11, close to GYRO. In this case, to account for all unstable modes or for the most unstable mode does not change the results.
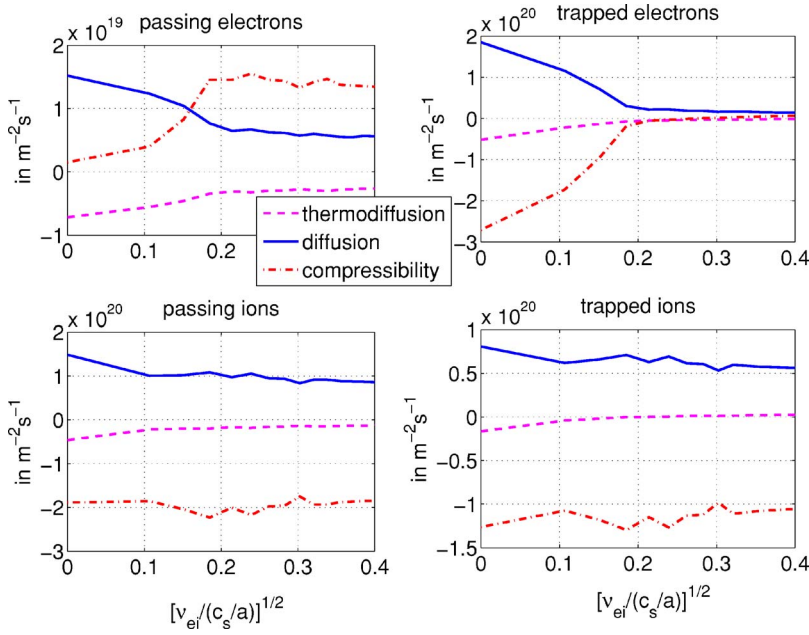
FIG. 10. (Color online) The flux due to the diffusion, the thermodiffusion, and the total compressibility for passing electrons, trapped electrons, passing ions, and trapped ions as a function of collisionality, computed with QuaLiKiz, for the case in which all unstable modes and the whole k_θ spectrum contribute.

A detailed analysis shows that, as expected, the flux driven by trapped electrons is responsible of this change of sign, see Fig. 10. And more interestingly, it shows that it is essentially due to a modified balanced between the inward compressibility, the inward thermodiffusion, and the diffusion terms, which all decrease as the collisionality increases, in favor of the outward diffusion. The balance leads to an outward electron flux at collisionality sensibly lower than the collisionality at which the diffusion and pinch terms decrease sensibly. The diffusion, thermodiffusion, and compressibility terms (respectively D_s, C_s^{th}, and C_s^c) for trapped and passing electrons and ions are plotted in Fig. 10.

APPENDIX C: ANALYTICAL DERIVATION OF THE QUASILINEAR CONVECTION TERMS

1. Convection terms in the case of curvature drift only

In this case, $n\Omega_s = -k_\theta T_s/(e_s BR)\xi(2-\lambda b)f(\lambda) = n\omega_{Ds}\xi(2-\lambda b)f(\lambda)$. To derive analytical expressions, we assume $\omega_{r0} \gg n\omega_{Ds}$, which is valid far from the instability threshold or for high Z_s trace impurities.

Thermodiffusion. The thermodiffusion term becomes

$$C_s^{\text{th}} = \left(\frac{q}{r}\right)^2 \frac{1}{B^2} \sum_{n,\omega} n^2 \left\langle \sqrt{\xi}e^{-\xi}\left(\xi - \frac{3}{2}\right)\right.$$
$$\left.\times \frac{\gamma_0}{[n\omega_{Ds}\xi(2-\lambda b)f(\lambda) - \omega_{r0}]^2 + \gamma_0^2}\right\rangle_{\xi,\lambda} |\tilde{\phi}_n|^2. \quad (C1)$$

For $\omega_{r0} \gg n\omega_{Ds}$, one gets

$$C_s^{\text{th}} \sim \left(\frac{q}{r}\right)^2 \frac{1}{B^2} \sum_{n,\omega} n^2 \left\langle \sqrt{\xi}e^{-\xi}\left(\xi - \frac{3}{2}\right)\left(\frac{\gamma_0}{\omega_{r0}^2 + \gamma_0^2}\right.\right.$$
$$\left.\left. + n\omega_{Ds}\xi(2-\lambda b)f(\lambda)\frac{2\omega_{r0}\gamma_0}{(\omega_{r0}^2+\gamma_0^2)^2}\right)\right\rangle_{\xi,\lambda} |\tilde{\phi}_n|^2$$
$$= \left(\frac{q}{r}\right)^2 \frac{1}{B^2} \sum_{n,\omega} n^2 \frac{3}{4}\sqrt{\pi}n\omega_{Ds}\frac{2\omega_{r0}\gamma_0}{(\omega_{r0}^2+\gamma_0^2)^2}\langle(2-\lambda b)f(\lambda)\rangle_\lambda |\tilde{\phi}_n|^2. \quad (C2)$$

The integral in energy, over ξ, would have been zero if the turbulence broadening function did not depend on energy. In this limit, and for the chosen frequency spectrum, the sign of thermodiffusion depends on the sign of the product $n\omega_{Ds}\omega_{r0}\langle(2-\lambda b)f(\lambda)\rangle_\lambda$. In the case of ion turbulence (electron turbulence), it is directed outward for ions (electrons) and inward for electrons (ions).[41] *Nota Bene* that the directions reverse if the magnetic shear is strongly negative or the MHD parameter, α, is large enough to reverse the sign of $\langle(2-\lambda b)f(\lambda)\rangle_\lambda$ from positive to negative.

For high Z_s trace impurities, the scaling with respect to the charge follows the $1/Z_s$ dependence as found previously.[18,20]

Compressibility. The compressibility term reduces to a curvature inward pinch,

$$RC_s^c = -\left(\frac{q}{r}\right)^2 \frac{1}{B^2} \sum_{n,\omega_0} n^2 \left\langle \xi^{3/2}e^{-\xi}(2\right.$$
$$\left. - \lambda b)f(\lambda)\frac{\gamma_0}{[n\omega_{Ds}\xi(2-\lambda b)f(\lambda) - \omega_{r0}]^2 + \gamma_0^2}\right\rangle_{\xi,\lambda} |\tilde{\phi}_n|^2. \quad (C3)$$

In the same limit as above, $\omega_{r0} \gg n\omega_{Ds}$, one gets

$$RC_s^c \sim -\left(\frac{q}{r}\right)^2 \frac{1}{B^2} \sum_{n,\omega_0} n^2 \left\langle \frac{3}{4}\sqrt{\pi}(2-\lambda b)f(\lambda)\left(\frac{\gamma_0}{\omega_{r0}^2+\gamma_0^2}\right.\right.$$
$$\left.\left. +\frac{5}{2}\frac{n\omega_{Ds}(2-\lambda b)f(\lambda)2\omega_{r0}\gamma_0}{(\omega_{r0}^2+\gamma_0^2)^2}\right)\right\rangle_\lambda |\tilde{\phi}_n|^2. \qquad (C4)$$

The first part of the energy integral is nonzero even in the case of no turbulence broadening. It does not depend on the charge nor does it reverse sign. It is always directed inward, unless s is strongly negative and/or α large enough to reverse the sign of $\langle(2-\lambda b)f(\lambda)\rangle_\lambda$, in which case the curvature convection can be directed outward. The second part exists only if a frequency spectrum model is taken into account. But it is of a lower order, so although it depends on the charge as $1/Z_s$, and reverses sign in the opposite manner compared to the thermodiffusion, this behavior does not affect the main feature.

2. Convection terms in the slab limit

Here, we consider the simpler slab limit, where the curvature is neglected, such that $n\Omega_s=k_\parallel V_\parallel \approx \pm k_\theta w(s/q)(V_{Ts}/R)\sqrt{\xi}$. We assume that $\omega \gg k_\parallel V_\parallel$, which is reasonable for heavy impurities, which have a lower thermal velocity, V_{Ts}, but rather a strong assumption for light ions and electrons, which have higher V_{Ts}.

Thermodiffusion. We then obtain for the thermodiffusion term

$$C_s^{th} \sim \left(\frac{q}{r}\right)^2 \frac{1}{B^2} \sum_{n,\omega_0} n^2 \left\langle \sqrt{\xi}e^{-\xi}\left(\xi-\frac{3}{2}\right)\right.$$
$$\times\left(\frac{\gamma_0}{\omega_{r0}^2+\gamma_0^2} \pm k_\theta w\frac{s}{q}\frac{V_{Ts}}{R}\omega_2(\lambda)\sqrt{\xi}\frac{2\omega_{r0}\gamma_0}{(\omega_{r0}^2+\gamma_0^2)^2}\right.$$
$$\left.\left. -\left(k_\theta w\frac{s}{q}\frac{V_{Ts}}{R}\right)^2\xi\frac{(2\omega_{r0})^2\gamma_0}{(\omega_{r0}^2+\gamma_0^2)^3}\right)\right\rangle_\xi |\tilde{\phi}_n|^2$$
$$= -\left(\frac{q}{r}\right)^2 \frac{1}{B^2} \sum_{n,\omega_0} n^2\frac{3}{4}\sqrt{\pi}\left\langle\left(k_\theta w\frac{s}{q}\frac{V_{Ts}}{R}\right)^2\right\rangle_\lambda \frac{(2\omega_{r0})^2\gamma_0}{(\omega_{r0}^2+\gamma_0^2)^3}|\tilde{\phi}_n|^2.$$
$$(C5)$$

Hence, in this limit, the thermodiffusion convection term is always inward. It scales as s^2 and as $1/A_s$ for trace impurities.

Compressibility. In the slab limit studied here, one obtains for the compressibility term

$$RC_s^c \sim -\left(\frac{q}{r}\right)^2 \frac{1}{B^2} \sum_{n,\omega_0} n^2 \left\langle \sqrt{\xi}e^{-\xi}\frac{\pm k_\theta w\dfrac{s}{q}\dfrac{V_{Ts}}{R}\sqrt{\xi}}{n\omega_{Ds}}\right.$$
$$\left.\times\left(\frac{\gamma_0}{\omega_{r0}^2+\gamma_0^2} \pm k_\theta w\frac{s}{q}\frac{V_{Ts}}{R}\omega_2(\lambda)\sqrt{\xi}\frac{2\omega_{r0}\gamma_0}{(\omega_{r0}^2+\gamma_0^2)^2}\right)\right\rangle_{\xi,\lambda} |\tilde{\phi}_n|^2$$
$$= -\left(\frac{q}{r}\right)^2 \frac{1}{B^2} \sum_{n,\omega_0} n^2\frac{3}{2}\sqrt{\pi}\frac{\left(k_\theta w\dfrac{s}{q}\dfrac{V_{Ts}}{R}\right)^2}{n\omega_{Ds}}\frac{\omega_{r0}\gamma_0}{(\omega_{r0}^2+\gamma_0^2)^2}|\tilde{\phi}_n|^2.$$
$$(C6)$$

Contrary to the curvature convection, and as the thermodiffusion, the parallel compressibility contributes to the flux only if one accounts for a frequency spectrum depending on energy, otherwise the energy integral in zero.

The sign of the parallel compressibility term depends both on the sign of the charge of the considered species and on the direction of the modes. For turbulence in the electron (ion) drift direction, the compressibility is directed inward for electrons (ions) and outward for ions (electrons). These directions are opposite to the thermodiffusion convection of trapped particles. This parallel compressibility term scales like Z_s/A_s, so at fixed mass, it is stronger for a higher charge species. These results were shown previously in Ref. 19.

[1] F. Jenko (private communication).
[2] F. Imbeaux (private communication).
[3] M. Kotschenreuther, W. Dorland, M. A. Beer, and G. W. Hammett, Phys. Plasmas **2**, 2381 (1995).
[4] R. E. Waltz, G. M. Staebler, W. Dorland, G. W. Hammett, M. Kotschenreuther, and J. A. Konings, Phys. Plasmas **4**, 2482 (1997).
[5] F. Jenko, T. Dannert, and C. Angioni, Plasma Phys. Controlled Fusion **47**, B195 (2005).
[6] G. M. Staebler, J. E. Kinsey, and R. E. Waltz, Phys. Plasmas **12**, 102508 (2005).
[7] Z. Lin, T. S. Hahm, W. W. Lee, W. M. Tang, and R. B. White, Science **281**, 1835 (1998).
[8] Z. Lin and T. S. Hahm, Phys. Plasmas **11**, 1099 (2004).
[9] V. Naulin, A. H. Nielsen, and J. Juul Rasmussen, Phys. Plasmas **12**, 122306 (2005).
[10] G. M. Staebler, J. E. Kinsey, and R. E. Waltz, Phys. Plasmas **14**, 055909 (2007).
[11] C. Bourdelle, X. Garbet, G. T. Hoang, J. Ongena, and R. V. Budny, Nucl. Fusion **42**, 892 (2002).
[12] T. Dannert and F. Jenko, Phys. Plasmas **12**, 072309 (2005).
[13] C. Angioni, A. G. Peeters, F. Jenko, and T. Dannert, Phys. Plasmas **12**, 112310 (2005).
[14] G. T. Hoang, C. Bourdelle, X. Garbet *et al.*, Phys. Rev. Lett. **90**, 155002 (2003).
[15] G. T. Hoang, C. Bourdelle, X. Garbet *et al.*, Phys. Rev. Lett. **93**, 135003 (2004).
[16] R. Guirlet, C. Giroud, T. Parisot, M. E. Puiatti, C. Bourdelle, L. Carraro, N. Dubuit, X. Garbet, and P. R. Thomas, Plasma Phys. Controlled Fusion **48**, B63 (2006).
[17] C. Giroud, C. Angioni, G. Bonheure *et al.*, "Progress in understanding of impurity transport at JET," *Proceedings of the 21st IAEA Fusion Energy Conference, Chengdu, 2006* (IAEA, Vienna, 2006), CD-ROM file EX8/3.
[18] X. Garbet, N. Dubuit, E. Asp, Y. Sarazin, C. Bourdelle, P. Ghendrih, and G. T. Hoang, Phys. Plasmas **12**, 082511 (2005).
[19] C. Angioni and A. G. Peeters, Phys. Rev. Lett. **96**, 095003 (2006).
[20] N. Dubuit, X. Garbet, T. Parisot, R. Guirlet, and C. Bourdelle, Phys. Plasmas **14**, 042301 (2007).
[21] M. Romanelli, G. Regnoli, and C. Bourdelle, Phys. Plasmas **14**, 082305 (2007).
[22] X. Garbet, L. Laurent, F. Mourgues, J. P. Roubin, and A. Samain, J. Comput. Phys. **87**, 249 (1990).
[23] M. Kotschenreuther, G. Rewoldt, and W. M. Tang, Comput. Phys. Commun. **88**, 128 (1995).
[24] J. Candy and R. E. Waltz, Phys. Rev. Lett. **91**, 045001 (2003).
[25] W. Horton, in *Handbook of Plasma Physics*, Basic Plasma Physics II, edited by A. A. Galeev and R. N. Sudan (Elsevier, New York, 1984), Vol. 2, p. 383.
[26] C. Bourdelle, G. T. Hoang, X. Litaudon, C. M. Roach, and T. Tala, for the ITPA Topical Group on Transport and ITB Physics, and the International ITB Database Working Group, Nucl. Fusion **45**, 110 (2005).
[27] P. Hennequin, C. Honoré, A. Truc, A. Quéméneur, F. Gervais, R. Sabot, and C. Fenzi, Plasma Phys. Controlled Fusion **46**, B121 (2004).
[28] G. R. McKee, C. C. Petty, R. E. Waltz *et al.*, Nucl. Fusion **41**, 1235 (2001).
[29] S. E. Parker, W. W. Lee, and R. A. Santoro, Phys. Rev. Lett. **71**, 2042 (1993).
[30] T. Dannert, Ph.D. thesis, Technische Universität München (2005); see

http://tumb1.biblio.tu-muenchen.de/publ/diss/ph/2005/dannert.pdf

[31] A. Hirose, S. Livingstone, and A. K. Singh, Nucl. Fusion **45**, 1628 (2005).

[32] T. F. R. Equipe, Phys. Fluids **25**, 641 (1983).

[33] A. J. Wootton, B. A. Carreras, H. Matsumoto, K. McGuire, W. A. Peebles, Ch. P. Ritz, P. W. Terry, and S. J. Zweben, Phys. Fluids B **2**, 2879 (1990).

[34] G. Antar, P. Devynck, C. Laviron *et al.*, Plasma Phys. Controlled Fusion **41**, 733 (1999).

[35] J. A. Krommes, "Statistical descriptions and plasma physics," in *Handbook of Plasma Physics*, edited by A. A. Galeev and R. N. Sudan (North-Holland, Amsterdam, 1984), Vol. 2, Chap. 5.5, p. 183.

[36] J. Weiland and H. Nordman, Phys. Fluids B **5**, 1669 (1993).

[37] A. Peeters, C. Angioni, and G. Tardini, C. R. Phys. **7**, 592 (2006).

[38] P. Hennequin, C. Honoré, A. Truc, A. Quéméneur, C. Fenzi-Bonizec, C. Bourdelle, X. Garbet, G. T. Hoang, and The Tore Supra Team, Nucl. Fusion **46**, S771 (2006).

[39] C. Angioni, A. G. Peeters, X. Garbet, A. Manini, and F. Ryter, and The ASDEX Upgrade Team, Nucl. Fusion **44**, 827 (2004).

[40] C. Bourdelle, Plasma Phys. Controlled Fusion **47**, A317 (2005).

[41] X. Garbet, L. Garzotti, P. Mantica, H. Nordman, M. Valovic, H. Weisen, and C. Angioni, Phys. Rev. Lett. **91**, 035001 (2003).

[42] C. Estrada-Mila, J. Candy, and R. E. Waltz, Phys. Plasmas **12**, 022305 (2005).

[43] H. Nordman, P. Strand, A. Eriksson, and J. Weiland, Plasma Phys. Controlled Fusion **47**, L11 (2005).

[44] M. B. Isichenko, A. V. Gruzinov, and P. H. Diamond, Phys. Rev. Lett. **74**, 4436 (1996).

[45] T. Parisot, R. Guirlet, C. Bourdelle, X. Garbet, N. Dubuit, F. Imbeaux, and P. R. Thomas, "Experimental impurity transport and theoretical interpretation in a Tore Supra lower-hybrid heated plasma," Plasma Phys. Controlled Fusion (submitted).